Medium and long period ground oscillatory pattern inferred by borehole tiltmetric data: new perspectives for the Campi Flegrei caldera crustal dynamics

E. De Lauro[1], S. Petrosino[2]*, C. Ricco[2], I. Aquino[2], M. Falanga[3]

[1]Università degli Studi di Roma Tre, Dipartimento di Architettura, Rome (Italy).

[2]Istituto Nazionale di Geofisica e Vulcanologia, Sezione di Napoli - Osservatorio Vesuviano, Naples (Italy).

[3]Università degli Studi di Salerno, Dipartimento di Ingegneria dell'Informazione ed Elettrica e Matematica applicata/DIEM, Fisciano (Italy).

Corresponding author: Simona Petrosino (simona.petrosino@ingv.it)

Abstract

We analyse tiltmetric time series recorded at borehole instruments recently installed at Campi Flegrei caldera (Italy), a volcanic area subjected to the phenomenon of bradyseism, which consists in fast ground uplift phases alternated to slow subsidence. For the first time, we evaluate the crustal response in terms of ground tilting of the entire caldera to external excitations such as long/medium-period tidal constituents, by adopting Independent Component Analysis. Indeed, we recognize diurnal (solar) and long-period (fortnightly and monthly) components, superimposed to the normal deformation trend of the area. They show well defined polarization directions and are associated with an oscillatory deformation pattern with the same periodicity of corresponding tidal constituents. The comparison with the local geology evidences that the tidal tilting is controlled by the local stress field distribution and the rheology, thus inducing structural and thermoelastic site effects.

Keywords: Tidal tilting, crustal response to earth tides, Campi Flegrei caldera

1 Introduction

A large number of geophysical time series often shows, superposed to the small time scale signals (seconds to hours), a periodical/quasi periodical behavior on long time scales that goes from semidiurnal up to seasonal/annual. Indeed, long-period amplitude variations have been observed in gravimetric data [Berrino and Corrado, 1991], ground deformation [Dong et al., 2002, Prawirodirdjo et al., 2006, Bottiglieri et al. 2007, 2010; Ben-Zion and Allarm, 2013], seismic noise [De Lauro et al., 2013; Hillers and Ben-Zion, 2011] and ocean tides [Capuano et al., 2011, 2012]. Cyclic patterns have also been found in earthquake triggering [e.g., McNutt and

Beaven, 1981; Bettinelli et al. 2008], seismic velocity changes [Hillers et al., 2015] and energy release [De Lauro et al., 2012a].

These variations are related to distinct mechanisms, often ascribed to rain and hydrologic phenomena [e.g., King et al., 2007], atmospheric pressure [e.g., van Dam et al., 2010], thermoelastic strain [Berger, 1975; Ben-Zion and Leary, 1986] and solid earth tides [Dong et al., 2002]. In many cases, long time series show a superposition of several effects ascribable to different external causes, which are considered as a background noise to be removed in order to isolate the non-seasonal processes related to the intrinsic crustal and source dynamics. This is particularly true in volcanic areas where the geophysical signals associated with the intrinsic dynamics (e.g. magmatic mass movement, pressure changes in the feeding system, inflation episodes, hydrothermal fluid migration) can be masked by such external “disturbances”.

On the other hand, rather than a disturbance to be removed, long-period modulations in geophysical time series can reveal significant information on the shallow earth structure, because they represent the response of the rocks to the stress field variation. Therefore, they can provide indications on the crustal stress state at depth, the rheology and the presence of inhomogeneities in the medium [Lambotte et al., 2006, Ben-Zion and Leary, 1986, Ben-Zion and Allarm, 2013], shedding light on the background state from which transient phenomena (such as tectonic and volcanic earthquakes, explosion-quakes, long-period events) can nucleate [see Hillers et al., 2015].

Moreover, tidal scale modulations of geophysical observables are also useful to infer significant information on the volcano source dynamics and for modeling the volcanic system [McNutt and Beaven, 1981]. For instance, De Martino et al. [2011a, 2011b] showed that the eruptions of Stromboli volcano were preceded by tidal precursors, linked to the duration of the eruptive episodes, which yield the Strombolian dynamics from the stationary phase towards the non-stationary state culminating with the eruptions. Additionally, De Lauro et al. [2012a, 2013] observed a diurnal modulation of the temporal energy release both of long continuous seismic data and of long-period (LP) events at Campi Flegrei (Italy), revealing the tidal influence on the mechanism of fluid charge/discharge in the branches of the hydrothermal system. Recently, the role of earth tides has also been recognized in modulating the occurrence of volcano-tectonic seismicity at Campi Flegrei, thus evidencing how exogenous phenomena contribute to the dynamics of the area (Petrosino et al., 2018).

Among the geophysical signals, tiltmetric measurements represent a useful tool for monitoring ground deformation in volcanic areas. However, as for other geodetic measurements [see, e.g., Dong et al., 2002; Bottiglieri et al., 2010], the tiltmetric recordings are affected by environmental factors (temperature, thermoelastic strain, atmospheric pressure), which have to be removed, or at least reduced, for improving the signal to noise ratio [Ricco et al., 2003]. The more the interesting signals are denoised from disturbances due to temperature, pressure, tides, etc., the more information can be extracted on the behavior of a volcano. Regarding the earth tides, of course, they affect the tiltmetric series with very strong contribution in the semidiurnal and diurnal bands. A first pre-filtering, indeed, removes those constituents to better focus the attention on the long-period components, which contain information about the trend of the tilting on the long time scale.

In the present paper, we investigate borehole tiltmetric series recorded at Campi Flegrei since their recent installation in March 2015. Compared with the signals recorded by surface sensors, the borehole installations are less affected by environmental factors such as temperature gradients, pressure, rainfall and variations in the aquifers, which can mask the actual deformation pattern.

The main aim of our work is to evaluate the effects of the long-period tidal external sources on the crustal area and to infer information on the medium response to that tidal loading from the tiltmetric data. To achieve that goal, we have developed a new approach based on an Independent Component Analysis [ICA; Hyvärinen and Oja, 2001] to identify the independent sources buried in the tiltmetric trend. In fact, techniques based on ICA have found relevant developments in geophysical applications and recently it has been successfully applied to obtain decomposition of seismic signals [Acernese et al., 2003; Capuano et al., 2016; Ciaramella et al., 2004, 2011; De Lauro et al., 2012a, 2012b, 2016; Capuano et al., 2017] as well as GPS time series [Bottiglieri et al. 2007, 2010, Gualandi et al., 2015, 2017], thus providing promising perspectives. Our analysis of the tiltmetric time series reveals that besides the trend related to the internal dynamics (ground deformation), the tiltmetric signals also contain tidal sources: i.e. diurnal (S1), luni-solar fortnightly (Mf) and lunar monthly (Mm). All these components show precise polarization directions, stable over the time, possibly conditioned by the local stress distribution and the geological features.

2 Tiltmetric Data at Campi Flegrei

The current tiltmetric monitoring network of Campi Flegrei [Ricco et al., 2003; Aquino et al., 2016] consists of ten stations: four surface short baselength platform AGI 702 tiltmeters [AGI, 1997], three AGI 722 tiltmeters installed in shallow wells, and three borehole digital Lily tiltmeters (HDM, ECO and CMP). The last new tiltmetric stations are equipped with digital sensors model “Lily Self-Leveling Borehole Tiltmeter” (Jewell Instruments ex AGI), instrumented with a self-levelling bubbles electrolyte on a range of ± 10 degrees, with a dynamic range of ± 330 μradians and a resolution less than 5 nradians. The tiltmeter package includes a magnetic compass and temperature sensor [Jewell Instruments, 2013]. Tiltmeters are installed into 25 meter deep boreholes to attenuate fluctuations of temperature of the ground's surface (Table 1). Ground tilt variations, recorded with a sampling frequency of 1 sample/minute (each sample is the mean value of 8000 acquisitions every 7.5 ms), are measured along two orthogonal directions aligned along the WE and NS axes. All the stations are distributed around the maximum ground uplift area (corresponding to the city of Pozzuoli) measured during the last three unrest episodes between 1969-1972, 1982-1984 and 2005-present by the periodical leveling surveys [Del Gaudio et al., 2010; D'Auria et al., 2011].

In this paper, we analyze the data from the borehole stations HDM, ECO and CMP (Figure 1, Table 1), which were installed in 2015, with the aim of studying more in detail the ongoing unrest phase at Campi Flegrei.

The time evolution of the deformation pattern at Campi Flegrei is reported in Figure 1: the curves originating from the three tiltmeters indicate the cumulative tiltmetric variation recorded since March 29, 2015 to December 31, 2016. The evolution of the deformation field is thus described by the tilt direction; a non-uniform ground uplift at Pozzuoli is reflected in a non-radial pattern. Moreover, the time series (Figure 1 and Figure 2) spanning 21 months show some anomalies on the EW components of two stations ECO and HDM.

Indeed, the latter recorded sharp changes in the tilting direction during the seismic swarm occurred on October 7, 2015; ECO drifted on the EW component on April 28, 2016 and this slow tilt lasted about 1 month, with a decrease of ≈ 0.05 ° C on the well temperature. To avoid contamination of the signals by these phenomena, the tiltmetric series were fragmented in order to have as long as possible continuous and contemporary recordings into three fixed time intervals: 3/29/2015÷9/30/2015 (I Period - PI), 10/30/2015÷4/15/2016 (II Period - PII) and 5/30/2016÷12/31/2016 (III Period - PIII). These intervals correspond to different rates of the vertical displacement derived from the GPS measurements at RITE station as shown in Table 2 (data taken from http://www.ov.ingv.it/ov/bollettini-mensili-campania/Bollettino Mensile Campi Flegrei 2017_09.pdf). From the data reported in Table 2, an overall slowly decreasing trend of the ground uplift velocity occur over the whole time span, although the rate of vertical displacement approaches to zero between the first and the second interval while it increases considerably between the second and the third interval.

3 Data Analysis: identification of the tidal components

We wish to quantify the long-period components in the tiltmetric data, because they can shed light on the vibration modes of the interested area, indicating the background state on which specific deformation trends (eventually due to the internal dynamics of the volcano) may superpose.

3.1 Harmonic analysis

It is well-known that the tiltmetric recordings are strongly affected by semidiurnal and diurnal tidal constituents [Sleeman et al., 2000]: indeed, the power spectrum of tiltmetric time series often shows large amplitude harmonics (such as M2, S2, S1 and K1), which are usually removed by filtering procedures before data processing [Ricco et al., 2003, 2007, 2013].

As a standard procedure, we first estimated both the barometric pressure and temperature contributions in our tiltmetric data, considering the pressure recorded by a station located in Solfatara and the temperature measured by the thermometers supplied with the borehole tiltmeters. The contributions resulted less than 3% and 0.5% of the variance, respectively, at the depths where the instruments are installed. Thus their effects are negligible in the tiltmetric time series and do not affect the tilt field at medium and long time scales (Ricco et al., 2007).

We performed a harmonic analysis in order to derive the main tidal constituents in the tiltmetric data. By using the T_Tide software [Pawlowicz et al., 2002], we estimated the amplitudes (and their uncertainties) of the tidal constituents on the EW and NS components of the unfiltered time series (Figure 2) recorded by the three tiltmeters. The observed amplitudes (Table 3) were then compared with the predicted ones retrieved by using GOTIC2 program (Matsumoto et al., 2001), by estimating the observed-to-predicted ratio for each constituents. For the diurnal and semidiurnal constituents we found average ratio values on the order of 2. The values are in agreement with those calculated for the O1 and M2 constituents using data from Michelson tiltmeters installed at Campi Flegrei (Amoruso et al., 2015). On the other hand, the average amplitude ratios for the long/medium period constituents (Mf and Mm) exceed about 15 and even 40 times those theoretically estimated. The observation of such anomalous high amplitude ratios suggests a possible amplification effect at long/medium period time scale in response to tidal forcing, that deserve further investigation. In order to improve the results of the harmonic analysis, more performing tools of inspection are needed, as we will discuss in the next section.

3.2 Independent Component Analysis

To gain more insight into the nature of the observed long/medium-period tidal constituents and better comprehend their effects on the tiltmetric series, we adopt an ICA based approach, aimed at the extraction of the statistically independent sources of deformation that generate the observed tilt data. The technique is based on a fourth-order statistics and makes decomposition of mixtures into independent time sources. The mixing model is written as $x_i = \sum_j^n a_{ij} s_j$, where $\boldsymbol{x}$ is an observed *m*-dimensional vector (tiltmetric recordings), **s** is an *n*-dimensional random vector whose components are assumed to be mutually independent; a_{ij} are the constant elements of an unknown *m x n* matrix **A** [Hyvärinen and Oja, 2001]. Specifically, we use the FastICA algorithm (available at the URL https://research.ics.aalto.fi/ica/fastica/), which seeks an orthogonal rotation of pre-whitened data, through a fixed-point iteration scheme, that maximizes a measure of non-Gaussianity of the rotated components. FastICA has the advantage to have a quadratic convergence, much faster than other approaches based on the linear convergence obtained by gradient methods.

A limitation of the technique is related to the number of extracted Independent Component (ICs) which is at maximum equal to the number of the input signals. If the number of independent sources is greater than the input signals, an optimal separation of the components is not guaranteed. Another drawback can arise by the presence of dominant sources in the original time series: in this case, some extractions can be redundant with the consequence of further decreasing the number of extracted ICs. In addition, whenever a source is dominant compared to the others, residual contributions can be often observed in the other extracted sources. Nevertheless, these shortcomings can be partially overcome by an appropriate pre-filtering procedure aimed at restricting the frequency band of analysis and possibly decreasing the number of independent sources in the original signals. The identification of non-redundant signals can be achieved by using Principal Component Analysis (PCA), a well-established method that reduces the dimensionality of the original data in such a way that the data variance in the lower dimensional space is maximized (Bishop, 1995; Hyvärinen et al., 2001). In this way, PCA is complementary to ICA, thus fixing the number of significant independent components to be extracted.

Indeed, the application of the ICA to our unfiltered tiltmetric dataset lead to a separation with dominant seasonal components mixed to long/medium-period and diurnal/semidiurnal ones. (Figure S1 in the Supplementary Material). In order to better focus on the sources of long/medium-period deformation, we filtered the detrended time series between 1-30 days by using a 3-pole butterworth filter. Then, for each sub-interval PI, PII and PIII, data were organized in a matrix, whose columns corresponds to the NS and EW component of each tiltmetric station; the dimension of the data matrix is *N*x6, where *N* is the number of points of the time series. In each sub-interval, the application of PCA leads us to identify three representative principal components retaining 90% of the information content. FastICA algorithm provides three non-redundant ICs characterized by well-defined dominant spectral peaks, reported in Table 4. As already mentioned, the ICA does not isolate the content of a single tidal constituent, hence some PSDs show multiple peaks; however, one dominant peak corresponding to a specific constituent is always enhanced in each IC.

Keeping in mind the Rayleigh criterion (Godin, 1972), two constituents are resolved if their frequencies, f_i and f_j, satisfy the relation $(f_i - f_j)\cdot t > R$, where t is the record length and R is the Rayleigh constant generally equal to 1. According to that criterion, the ICs with monthly periodicity are compatible with the lunar monthly Mm (T=27.55 days) and those with fortnightly period are related to the lunar fortnightly Mf (T=13.66 days). Moreover, some ICs with period of nearly 18 days (not ascribable to any tidal constituent) are also extracted. Regarding the ICs with diurnal periodicity, it is important to note that the length of the time recordings allows to resolve between solar and lunar contribution. On this basis, the extracted ICs with period of exactly 24h correspond to the solar diurnal S1.

In order to highlight the relevant information extracted by ICA, the attention is focused on the non-redundant ICs (Figure 3), which were selected on the basis of their spectral content among those obtained for the sub-intervals PI, PII and PIII. To summarize, considering the union of all the extracted components over the three time intervals PI, PII and PIII, we have in total four ICs: three effective tidal constituents (Mm, Mf, S1) plus a 18-day component (Figure 3). The latter is likely to be ascribed to residual barometric pressure variations, related to the air circulation and planetary waves (such as Rossby waves) in the atmosphere [see, e.g., Campello et al., 2004, López-González et al., 2009]. Indeed, the spectrum of the pressure time series detected at a barometer located in Solfatara area shows a nearly 18-day periodicity, as shown in Figure S2 of the Supplementary Material.

An interesting observation regards the seasonality of the different ICs over the three periods. In particular, PI that mainly corresponds to spring and summer time is characterized by a strong solar, diurnal contribution and by monthly constituents. A similar consideration also holds for PIII (which encompasses spring and summer time, plus some winter months). On the contrary, in PII (autumn and winter period) mostly fortnightly (Mf) constituent appears. A check performed by applying ICA to the entire time record (21 months), in order to increase the temporal resolution confirms that the extracted ICs correspond to the Mm, 18-day and S1; in this case, the Mf is not extracted, probably masked by the large amplitude constituents Mm and S1 throughout the considered interval. The results are shown in Figure S3 of the Supplementary Material.

To get more insight on the nature of the observed tidal components, the tiltmetric time series were narrow-band filtered in the frequency bands corresponding to the ICs. The starting three bands were centered on the frequency of the extracted tidal constituents (Mm, Mf and S1), then the filter boundaries were optimized by iteratively maximizing the correlation function between the ICs and the filtered series [Acernese et al., 2004; De Lauro et al., 2009, 2012b]. The iteration procedure was carried on until the correlation coefficient reaches a values of 0.9; it generally took a few iterations. The obtained signals narrow-band filtered around the peaks of the independent sources can be considered as the tiltmetric "image" of the ICs (Figure 4). As expected, the S1 component shows an amplitude modulation on a seasonal scale (i.e. it attains the maximum amplitude in PI and PIII), particularly evident at the CMP tiltmeter. Instead, no evident seasonal amplitude variation occurs at HDM site. The difference in the amplitudes at the three stations could be indicative of a sort of "site effect" (e.g. the three sites have different response to the external S1 source).

3.3 Diurnal and long-period tilt pattern

To investigate the pattern related to the extracted tidal constituents, we estimated the azimuth of the tilt vector corresponding to the filtered signals at each site for both the three sub-intervals (PI, PII and PIII) and the entire period. The azimuth (clockwise from the North) were evaluated over sliding time windows with length equal to the period of each tidal constituents and overlap of 88% for the Mm and Mf, and 50% for the S1.

The resulting values range in a narrow interval (Figure 5), indicating that the ground tilt occurs on preferential planes with an oscillatory pattern, which depends on the periodicity of the corresponding tidal constituent. In particular, for the Mm and Mf constituents, at HDM and CMP tiltmeters, the azimuth directions (ESE-WNW and nearly E-W) remain roughly constant and almost parallel throughout the entire period of observation of 21 months. At ECO site the ground tilt has an average NE-SW azimutal direction. At a shorter time-scale, a difference of about 60° of the azimuth value is observed during PII (compared to PI and PIII). Regarding the diurnal S1, at CMP and ECO sites the azimuths are almost constant, (E-W and NE-SW respectively). At HDM a slight azimuth variation (30-40°) between PI-III e PII is observed; the dominant direction over the 21 months is NW-SE.

The W-E and S-N components of the three extracted tidal constituents are combined into a vectorial plot of the tilt variation over the time. The least-squares best fit of the particle motion thus obtained identifies the predominant directions along which the ground tilts with diurnal, fortnightly and monthly periodicity. The resulting tiltmetric vectors for the three tidal constituents are shown on the map of Figure 6: the Mm tilting amplitude is more than twice the Mf both at CMP and HDM and, as already discussed in Section 2.2 (Figure 4), the S1 amplitude is maximum at CMP and minimum at HDM. For all the three constituents, the tilt direction of ECO forms an angle of about 40-60° with those of CMP and HDM.

4 Discussions and Conclusions

In the present paper, we apply the ICA to tiltmetric recordings and demonstrate its ability in successfully separating the tidal contributions with different periodicity in the original signals. As shown by Bottiglieri et al. [2007, 2010] and by Gualandi et al. [2015] who analysed geodetic GPS time series, our results confirm how powerful the method is for treating tilmetetic data too.

Our application of ICA to the borehole tilmetric time series at Campi Flegrei reveals the ground tilt response to diurnal, fortnightly and monthly tidal deformations. In other words, the astronomical earth tides have an effect on a large area of the caldera, inducing ground oscillations with the same periodicity of the tidal constituents. These oscillations are “captured” by the borehole tiltmeters as a ground tilting along well defined planes with nearly a constat orientation.

We find evidence that the general directions of the tilting planes is constrained by the local stress field. Indeed, from the study of the distribution and orientation of faults and fractures, a complex pattern of the stress field at Campi Flegrei caldera emerges [Vitale and Isaia, 2014]. In particular, in the center sector, the fracture orientations are roughly NE–SW and NW–SE, and the faults indicate a predominant NNE–SSW extensive regime (see Figure 10 in Vitale and Isaia, 2014). Despite the relative proximity, the tilmetric stations are installed in three sites characterized by a distinct local kinematics. CMP is located in the area of La Starza, a marine terrace that is the most uplifted part of the caldera floor, and it is affected by both NNE–SSW and NW–SE extensive regimes. ECO is situated between La Starza and the Solfatara crater, in a sector characterized by many faults with dominant NNE–SSW extensive regime. HDM is installed at the Accademia site, above the Mt. Olibano lava dome, which bounds the south Solfatara crater. Here, a complex pattern of faults related to both the local stress and the deformation of the resurgent dome leads to the coexistence of NNE–SSW and NW–SE extensive kinematics. It is worth to note that the tilt planes orientation retrieved from our analysis are right along the directions of the extensional axis corresponding to the local stress field. In other words, the oscillations of the tilting planes at tidal scales thus occur along pre-existing structural features and their orientation is conditioned by the local stress field.

A support for this hypothesis comes from the comparison between the experimental data and the theoretical tilt calculated by using the code GOTIC2, considering both solid earth tides and ocean loading. Indeed, for the long-period constituents, the orientation of the synthetic tilt is independent of the sites. We remark that the codes generating theoretical tides do not take into account the site effects related to the medium/small scale geological structures. In fact, it has been demonstrated that the theoretical tides can differ up to 30-50% from those observed, due to both inaccuracy of the tidal models and/or rock properties at the site [Langbein, 2010, Kohl and Levine, 1995]. Even more so, the deviation of the tilting azimuths from the theoretical directions we observed suggests the occurrence of a site effect.

We further recognize that the local geology also plays an important role in modulating the amplitude of the tidal constituents detected in the tiltmetric time series. Indeed, the diurnal S1 constituent, which is strictly related to the insolation, induces a thermoelastic strain, whose propagation at depth is controlled by the rheology. The proposed model predicts that this strain is greater for unconsolidated heterogeneus materials [Berger, 1975; Ben-Zion and Leary, 1986]. The stratigraphy, derived (down to a depth of about 25 m) during the drilling operations at Campi Flegrei, shows that : a) CMP site is characterized by layers of sands alternated to ashes and pyroclastics; b) ECO site is composed by a sequence of pyroclastic deposits with various granulometry; c) HDM site shows pyroclastics and sands intercalated to lava layers with thicknesses of about 4-5 m [Aquino et al., 2016]. In the framework of the thermoelastic model, the loose and unconsolidated soils of CMP and ECO sites would thus cause the observed amplification of the diurnal S1 constituent, while the harder materials such as lava rocks at HDM would act as a damper.

In conclusion, we have evidenced that at Campi Flegrei the tidal forces induce an oscillatory deformation pattern superimposed to the normal trend related to endogenous phenomena. The orientation and amplitude of the “tidal” tilting are in turn controlled by the local stress field, the pre-existing structures and the local rheology, thus leading to “structural and thermoelastic” site effects. A better understanding of these effects on the tiltmetric recordings can help in:

1) improving the outline of the local geology (which is also useful to individuate the better sites for future instruments installation).
2) allowing the calculation of the thermal admittance, whose estimate is necessary to remove the thermal contribution from the tiltmetric signals.
3) focusing on the internal sources after the removal of the external tidal effects, thus allowing a better comprehension of the volcanic dynamics of Campi Flegrei caldera.
4) modelling the coupling mechanism between ground deformation and earth tides.

Our results suggest that routine analysis of tiltmeter data by ICA provides additional information on deformation patterns that can be overlooked by classical analysis. More in general, the ICA is able to extract the crustal response to the tidal forces, which is controlled by the fault orientation and the rheology. Therefore variations of the local stress field and/or the rheology, possibly induced by magmatic or hydrothermal fluid movements can cause changes in the oscillatory pattern of the deformation. Tiltmeters and strainmeters have potentially high sensitivity in detecting ground deformation variations (Amoruso et al., 2015); in this framework, the use of ICA of tiltmetric time series can help in detecting such changes and in monitoring ongoing unrest phases in volcanic areas.

Acknowledgments

Harmonic analysis has been performed by using T_Tide software [Pawlowicz et al., 2002]. For the Independent Component Analysis the FastIca package vailable at the URL https://research.ics.aalto.fi/ica/fastica/ was used. Finally, we thank an anonymous Reviewer for having provided the estimates of the theoretical tidal amplitudes, and Pierpaolo Pappacena for his help in composing Figure 5.

References

Acernese, F., Ciaramella, A., De Martino, S., De Rosa, R., Falanga, M., Tagliaferri, R. (2003), Neural networks for blind-source separation of Stromboli explosion quakes, IEEE Trans. Neural Networks, 14, 167–175.

Acernese, F., Ciaramella, A., De Martino, S., Falanga, M., Godano, C., Tagliaferri, R. (2004), Polarisation analysis of the independent components of low frequency events at Stromboli volcano (Eolian Islands, Italy). *J. Volcanol. Geotherm. Res.*, 137(1-3), 153-168.

AGI, (1997), 700-Series platform and surface mount tiltmeters. User’s Manual, *User’s Manual no. B-88-1016, Rev. E.*

Amoruso, A., Crescentini, L., Scarpa, R., Bilham, R., Linde, A. T., Sacks, I. S. (2015), Abrupt magma chamber contraction and microseismicity at Campi Flegrei, Italy: Cause and effect determined from strainmeters and tiltmeters. *Journal of Geophysical Research: Solid Earth*, 120(8), 5467-5478.

Aquino, I., Ricco, C., Del Gaudio, C., Augusti, V., Scarpato, G. (2016), Potenziamento delle Reti Tiltmetriche nell’area vulcanica campana: Rapporto sull’attività svolta nell’ambito del progetto vulcamed. *Rapporti Tecnici INGV*, 348, ISSN 2039-6651 348.

Ben-Zion, Y., & Leary, P. (1986), Thermoelastic strain in a half-space covered by unconsolidated material. *Bulletin of the Seismological Society of America*, 76 (5), 1447–1460.

Ben-Zion, Y., & Allam, A. A. (2013), Seasonal thermoelastic strain and postseismic effects in Parkfield borehole dilatometers. *Earth Planet. Sci. Lett.*, 379, 120–126.

Berger, J. (1975), A note on thermoelastic strains and tilts. *J. Geophys. Res.*, 80(2), 274–277. doi:10.1029/JB080i002p00274

Berrino, G., Corrado, G. (1991), Tidal signal in the recent dynamics of Campi Flegrei caldera (Italy). *J. Volcanol. Geotherm. Res.*, 48, 93–101.

Bettinelli, P., Avouac, J. P., Flouzat, M., Bollinger, L., Ramillien, G., Rajaure, S., Sapkota, S. (2008), Seasonal variations of seismicity and geodetic strain in the Himalaya induced by surface hydrology. *Earth Planet. Sci. Lett*., 266(3–4), 332–344. https://doi.org/10.1016/j.epsl.2007.11.021

Bishop, C.M. (1995), Neural Networks for Pattern Recognition. Oxford University Press.

Bottiglieri, M., Falanga, M., Tammaro, U., Obrizzo, F., De Martino, P., Godano, C., and Pingue, F. (2007), Independent component analysis as a tool for ground deformation analysis. *Geophysical Journal International*, 168(3), 1305-1310.

Bottiglieri, M., Falanga, M., Tammaro, U., De Martino, P., Obrizzo, F., Godano, C., Pingue, F. (2010), Characterization of GPS time series at the Neapolitan volcanic area by statistical analysis. *Journal of Geophysical Research: Solid Earth*, 115(B10).

Campello, F. D., Saraiva, J., Krusche, N. (2004), Periodicity of atmospheric phenomena occurring in the extreme South of Brazil. *Atmospheric science letters*, 5(1-4), 65-76.

Capuano, P., De Lauro, E., De Martino, S., Falanga, M. (2011), Water-level oscillations in the Adriatic Sea as coherent self-oscillations inferred by independent component analysis. *Progress in oceanography*, 91(4), 447-460. doi:10.1016/j.pocean.2011.06.001.

Capuano, P., De Lauro, E., De Martino, S., Falanga, M. (2012), Observations of the 18.6-year cycle effects on the sea-level oscillations in the North Atlantic Ocean. *Europhys. Lett.*, 100, 39003, 1–6. doi:10.1209/0295-5075/100/39003.

Capuano, P., De Lauro, E., De Martino, S., Falanga, M. (2016), Detailed investigation of Long-Period activity at Campi Flegrei by Convolutive Independent Component Analysis. *Phys. Earth Planet. Int.*, 253, 48-57.

Capuano, P., De Lauro, E., De Martino, S., Falanga, M., Petrosino, S. (2017), Convolutive independent component analysis for processing massive datasets: a case study at Campi Flegrei (Italy). *Natural Hazards*, 86(2), 417-429. 10.1007/s11069-016-2545-0.

Ciaramella, A., De Lauro, E., De Martino, S., Di Lieto, B., Falanga, M., Tagliaferri, R. (2004), Characterization of Strombolian events by using independent component analysis. *Nonlinear Processes in Geophysics*,11, 453-461.

Ciaramella, A., De Lauro, E., Falanga, M., Petrosino, S. (2011), Automatic detection of long-period events at Campi Flegrei Caldera (Italy), *Geophys. Res. Lett.*, 38, L18302. doi:10.1029/2011GL049065

D'Auria, L., Giudicepietro, F., Aquino, I., Borriello, G., Del Gaudio, C., Lo Bascio, D., Martini, M., Ricciardi, G. P., Ricciolino P., Ricco, C. (2011), Repeated fluid-transfer episodes as a mechanism for the recent dynamics of Campi Flegrei caldera (1989–2010). *J. Geophys. Res.*, 116, B04313, doi:10.1029/2010JB007837

De Lauro, E., De Martino, S., Falanga, M., Palo, M. (2009), Modelling the macroscopic behavior of Strombolian explosions at Erebus volcano. *Phys. Earth Planet. Int.* 176(3-4), 174–186.

De Lauro, E., Falanga, M., Petrosino, S. (2012a), Study on the long-period source mechanism at Campi Flegrei (Italy) by a multi-parametric analysis. *Phys. Earth Planet. Int*., 206-207, 16–30. http://dx.doi.org/10.1016/j.pepi.2012.06.006

De Lauro, E., De Martino, S., Palo, M., Ibañez, J. M. (2012b). Self-sustained oscillations at Volcán de Colima (México) inferred by independent component analysis. *Bulletin of Volcanology*, *74*(1), 279-292.

De Lauro, E., De Martino, S., Falanga, M., Petrosino, S. (2013), Synchronization between tides and sustained oscillations of the hydrothermal system of Campi Flegrei (Italy). *Geochemistry, Geophysics, Geosystems*, 14(8), 2628-2637.

De Lauro, E., De Martino, S., Falanga, M., Petrosino, S., (2016). Fast wavefield decomposition of volcano-tectonic earthquakes into polarized P and S waves by Independent Component Analysis. *Tectonophysics*, 690, 355-361. https://doi.org/10.1016/j.tecto.2016.10.005

Del Gaudio, C., Aquino, I., Ricciardi, G. P., Ricco, C., Scandone, R. (2010), Unrest episodes at Campi Flegrei: A reconstruction of vertical ground movement s during 190 5–2009. *J. Volcanol. Geother m. Res*., 195(1), 48–56. doi:10.1016/j.jvolgeores.2010.05.014

De Martino, S., Palo, M., Cimini, G. B. (2011a), A statistical study of the Stromboli volcano explosion quakes before and during 2002–2003 eruptive crisis. *J. Geophys. Res.*, 116, B04303, doi:10.1029/2010JB008047

De Martino, S., Falanga, M., Palo, M., Montalto, P., Patané, D. (2011b), Statistical analysis of the volcano seismicity during the 2007 crisis of Stromboli, Italy. *J. Geophys. Res.*, 116, B09312, doi:10.1029/2010JB007503

Dong, D., Fang, P., Bock, Y., Cheng, M. K., Miyazaki, S. (2002), Anatomy of apparent seasonal variations from GPS-derived site position time series. *J. Geophys. Res.*, 107(B4), 2075. doi:10.1029/2001JB000573

Gualandi, A., Serpelloni, E., Belardinelli, M. E. (2015). Blind source separation problem in GPS time series. *Journal of Geodesy*, 90(4), 323-341. doi:10.1007/s00190-015-0875-4

Gualandi, A., Nichele, C., Serpelloni, E., Chiaraluce, L., Anderlini, L., Latorre, D., Belardinelli, M. E., Avouac, J.-P. (2017), Aseismic deformation associated with an earthquake swarm in the northern Apennines (Italy), *Geophys. Res. Lett.*, 44, 7706–7714, doi:10.1002/2017GL073687

Godin, G. (1972), The Analysis of Tides. University of Toronto Press, 264 pp.

Hillers, G. & Ben-Zion, Y. (2011), Seasonal variations of observed noise amplitudes at 2-18 Hz in southern California, *Geophys. J. Int.*, 184, 860–868, doi: 10.1111/j.1365-246X.2010.04886.x

López-González, M. J., Rodríguez, E., García-Comas, M., Costa, V., Shepherd, M. G., Shepherd, G. G., Aushev, V. M., Sargoytchev, S. (2009), Climatology of planetary wave type oscillations with periods of 2-20 days derived from O2 atmospheric and OH (6-2) airglow observations at mid-latitude with SATI. *Ann. Geophys.*, 27, 3645 – 3662.

Hillers, G., Retailleau, L., Campillo, M., Inbal, A., Ampuero, J.-P., Nishimura, T. (2015), In situ observations of velocity changes in response to tidal deformation from analysis of the high-frequency ambient wavefield. *J. Geophys. Res.*, 120,210–225.

Hyvärinen, A., Karhunen, J., Oja, E. (2001), Independent Component Analysis. Series on Adaptive and Learning Systems for Signal Processing, Communications, and Control.

Jewell Instruments, (2013), LILY Self-Leveling Borehole Tiltmeter, *User's Manual, no. B-05-1003, Rev. G.*

King, N. E., Argus, D., Langbein, J., Agnew, D. C., Bawden, G., Dollar, R. S., Liu, Z., Galloway, D., Reichard, E., Yong, A., Webb, F. H., Bock, Y., Stark, K., Barseghian, D., (2007), Space geodetic observation of expansion of the San Gabriel Valley, California, aquifer system, during heavy rainfall in winter 2004–2005. *J. Geophys. Res.*, 112, B03409. doi:10.1029/2006JB004448

Kohl, M. L., & Levine, J. (1995). Measurement and interpretation of tidal tilts in a small array. *Journal of Geophysical Research: Solid Earth*, 100(B3), 3929-3941.

Lambotte, S., Rivera, L., Hinderer, J. (2006), Vertical and horizontal seismometric observations of tides. *Journal of Geodynamics*, 41(1–3) 39–58. https://doi.org/10.1016/j.jog.2005.08.021

Langbein, J. (2010), Effect of error in theoretical Earth tide on calibration of borehole strainmeters. *Geophysical Research Letters*, *37*(21).

Matsumoto, K., Sato, T., Takanezawa, T., and Ooe, M. (2001), GOTIC2: A Program for Computation of Oceanic Tidal Loading Effect, *J. Geod. Soc. Japan*, 47, 243-248.

McNutt, S.R., Beavan, R.J. (1981), Volcanic earthquakes at Pavlof volcano correlated with the solid earth tide. *Nature* 294, 615–618.

Pawlowicz, R., Beardsley, B., Lentz, S. (2002), Classical tidal harmonic analysis including error estimates in MATLAB using T_TIDE. *Computers & Geosciences*, 28(8), 929-937.

Prawirodirdjo, L., Ben-Zion, Y., Bock, Y. (2006), Observation and modeling of thermoelastic strain in Southern California Integrated GPS Network daily position time series. *J. Geophys. Res.*, 111, B02408. doi:10.1029/2005JB003716

Petrosino, S., Cusano, P., Madonia, P. (2018), Tidal and hydrological periodicities of seismicity reveal new risk scenarios at Campi Flegrei caldera. *Scientific Report*, 8:13808, doi:10.1038/s41598-018-31760-4.

Ricco, C., Aquino, I., Del Gaudio, C. (2003), Ground tilt monitoring at Phlegraean Fields (Italy): a methodological approach. *Annals of Geophysics*, 46(6), 1297–1314.

Ricco, C., Aquino, I., Borgstrom, S. E., Del Gaudio, C. (2007), A study of tilt change recorded from July to October 2006 at the Phlegraean Fields (Naples, Italy). *Annals of Geophysics*, 50, 661–674.

Ricco, C., Aquino, I., Borgstrom, S. E. P., Del Gaudio, C. (2013), 19 years of tilt data on Mt. Vesuvius: state of the art and future perspectives. *Annals of Geophysics*, 56(4), S0453. doi:10.4401/ag-6459.

Sleeman, R., Haak, H. W., Bos, M. S., Van Gend, J. J. A. (2000), Tidal tilt observations in the Netherlands using shallow borehole tiltmeters. *Physics and Chemistry of the Earth, Part A: Solid Earth and Geodesy*, 25(4), 415-420.

van Dam, T., Altamimi,*Z.*, Collilieux, X., Ray, J. (2010), Topographically induced height errors in predicted atmospheric loading effects. *J. Geophys. Res.,* 115, B07415. doi:10.1029/2009JB006810.

Vitale, S., & Isaia, R. (2014), Fractures and faults in volcanic rocks (Campi Flegrei, southern Italy): Insight into volcano-tectonic processes. *International Journal of Earth Sciences*, 103, 801–819. doi: 10 .1007/s00531 -013 -0979 -0

Tilt Station	Height a.m.s.l. m	Depth m	UTM N m	UTM E m
CMP	62	-24.5	4520828	33T 425228
ECO	89	-24.8	4520474	33T 426646.4
HDM	112	-25.9	4519117	33T 427424

Table 1. Geographical positions of the borehole tiltmeters.

3/29/2015÷9/30/2015 I Period	I÷II	10/30/2015÷4/15/2016 II Period	II÷III	5/30/2016÷12/31/2016 III Period
6.73 mm/month	0.0 mm/ month	6.18 mm/ month	13.34 mm/ month	4.51 mm/ month

Table 2. GPS Station RITE (Pozzuoli, Rione Terra): rates of the vertical displacement.

Tidal Constituent	Amplitude (μr) CMP NS	Amplitude (μr) CMP EW	Amplitude (μr) ECO NS	Amplitude (μr) ECO EW	Amplitude (μr) HDM NS	Amplitude (μr) HDM EW	Pred. Amplitude (μr) NS	Pred. Amplitude (μr) EW
Mm	0.0347 ± 0.004	0.1027 ± 0.005	0.0574 ± 0.004	0.1485 ± 0.019	0.0465 ± 0.002	0.0624 ± 0.005	0.0036	0.0003
Mf	0.0286 ± 0.004	0.0758 ± 0.005	0.0229 ± 0.003	0.1339 ± 0.016	0.0200 ± 0.002	0.0355 ± 0.005	0.0067	0.0004
O1	0.0076 ± 0.004	0.0135 ± 0.006	0.0122 ± 0.005	0.0176 ± 0.020	0.0083 ± 0.003	0.0158 ± 0.007	0.0045	0.0155
S1	0.0180 ± 0.005	0.1673 ± 0.006	0.0928 ± 0.006	0.1135 ± 0.026	0.0292 ± 0.004	0.0195 ± 0.007	-	-
K1	0.0080 ± 0.004	0.0738 ± 0.006	0.0291 ± 0.003	0.0222 ± 0.022	0.0433 ± 0.003	0.0094 ± 0.005	0.0090	0.0213
M2	0.0540 ± 0.004	0.0341 ± 0.004	0.0610 ± 0.003	0.0332 ± 0.019	0.1382 ± 0.002	0.0086 ± 0.005	0.0279	0.0297

Table 3. Observed and predicted amplitudes of the tidal constituents on the NS and EW components of the three tiltmeters. Predicted amplitudes are estimated by means of GOTIC2 including the ocean loading, and averaged over the three sites.

Time interval	IC_1 period (days)	TC	IC_2 period (days)	TC	IC_3 period (days)	TC
I	**26.6**	**Mm**	**18.6**	**-**	**1.0**	**S1**
II	**24.1**	**Mm**	**18.8**	**-**	**14.1**	**Mf**
III	**28.7**	**Mm**	**20.1**	**-**	**1.0**	**S1**

Table 4. Main spectral peaks of the ICs obtained for the three investigated time intervals (PI, PII PIII) and likely associated with a tidal constituent (TC). The different colors indicate the association with the ICs shown in Figure 3.

Figure Captions

Figure. 1 Map of the Campi Flegrei caldera, superimposed on a grid representing the two-dimensional plane of ground inclinations, in which each mesh is equivalent to a tiltmetric variation of 20 μradians over a distance of 1 km. The three sites CMP, ECO and HDM are distinguished by different colors (red, green and blue, respectively), as well as the curves that originate from them: the latter indicate the cumulative tiltmetric variation recorded since March 29, 2015 to December 31, 2016. Squares and full circles superimposed on the cumulative tilt variation curves, mark the start and the end, respectively, of the ground tilt occurred in the three analysed periods.

Figure 2. Ground tilt recorded at CMP, ECO and HDM tiltmeters in 644 days elapsed since 2015/01/01: the colors identify different sensors, dotted and bold lines indicate the NS, EW components, respectively. The tilt increase on S-N component corresponds to Northward down with respect to the site station, while the tilt increase on W-E component corresponds to Eastward down. The signals are also segmented into three time intervals characterized by different kinematic behaviors.

Figure 3. An example of the four non-redundant ICs selected among those obtained by applying FastICA to the time sub-intervals PI, PII and PIII. The time history (on the left) of each ICs is reported to a common origin chosen as zero; the duration is expressed in days. The corresponding power spectral density PSD is shown (on the right). Different colors are associated to the tidal constituents Mm (ocre), Mf (cyan) and S1 (magenta) listed in Table 4. The

18-day component, possibly ascribed to medium and long-period variations of the barometric pressure, is represented in gray. The dashed lines in the PSD plots correspond to the frequencies of the three tidal constituents and the 18-day component.

Figure 4. Tiltmetric signals filtered in the frequencies bands corresponding to the ICs. Different colors indicate the tidal constituents Mm (ocre), Mf (cyan) and S1 (magenta). The x axis reports the days elapsed since 2015/01/01.

Figure 5. (**a**) Rose diagrams of the azimuths of the tiltmetric signals corresponding to the Mm constituent (red = CMP, green = ECO, blue = HDM). Each column represents the results obtained for the different time intervals (PI, PII, PIII, and the entire period of 21 months); (**b**) the same for the Mf constituent; (**c**) the same for the S1 constituent.

Figure 6. Map of the Campi Flegrei caldera, superimposed on a grid representing the two-dimensional plane of ground inclinations in which each mesh is equivalent to a tiltmetric variation of 0.1 μradians over a distance of 1.5 km. The three sites CMP, ECO and HDM are distinguished by different colors (red, green and blue, respectively). For each of them, the predominant directions along which the ground tilt with monthly (ocre), fortnightly (cyan) and diurnal (magenta) period are represented.

Figure 1
Click here to download high resolution image

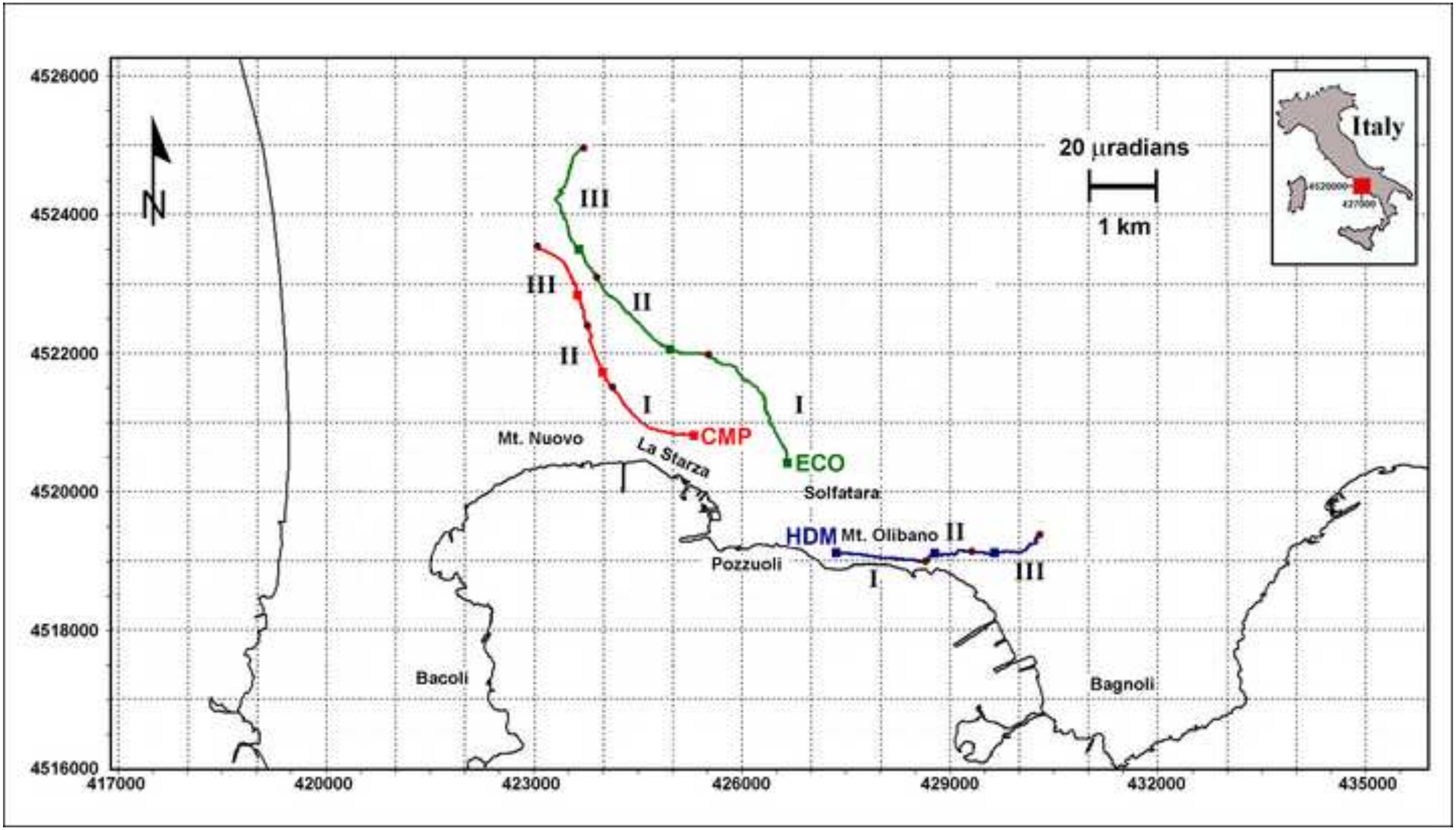

Figure 2

Click here to download high resolution image

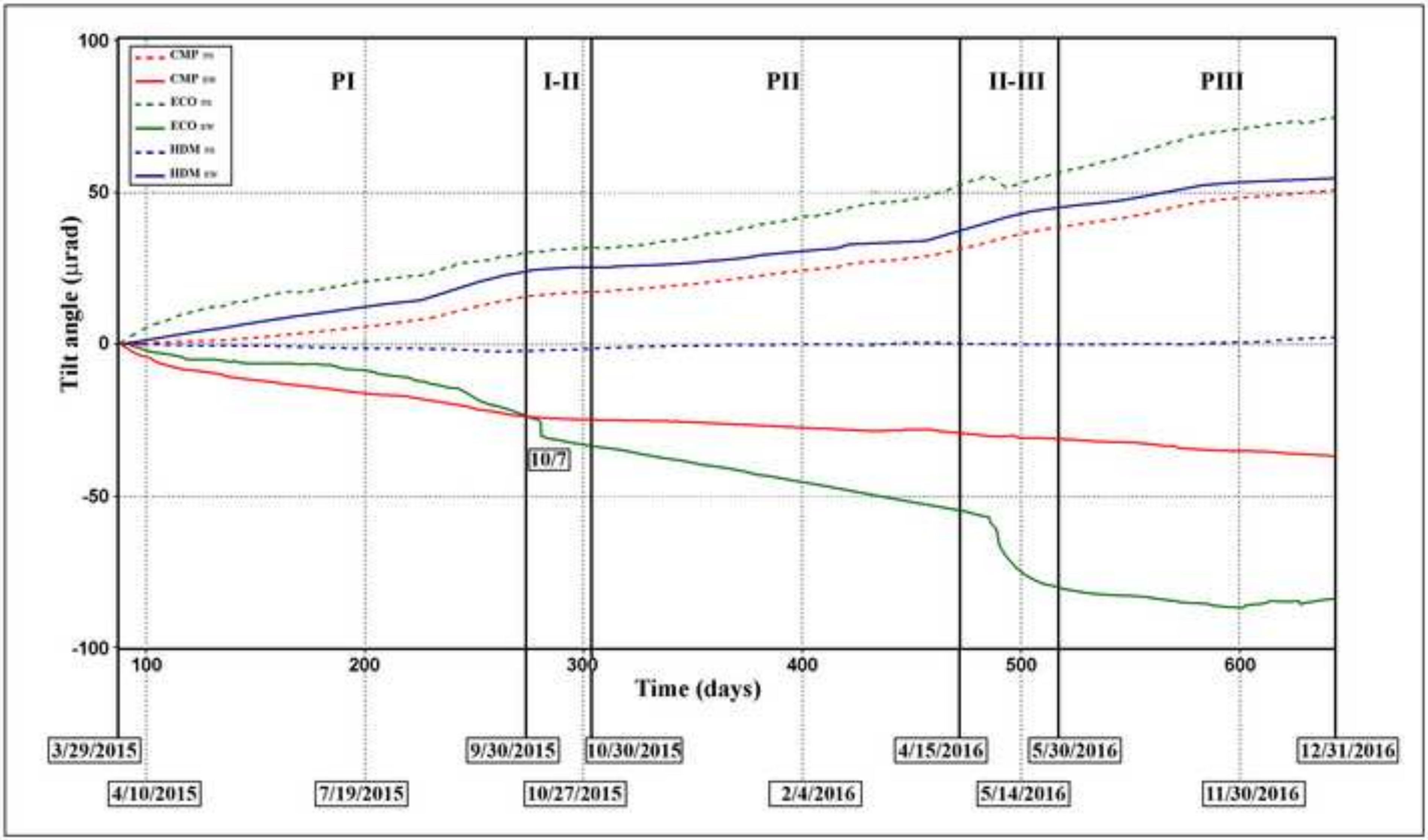

Figure 3
Click here to download high resolution image

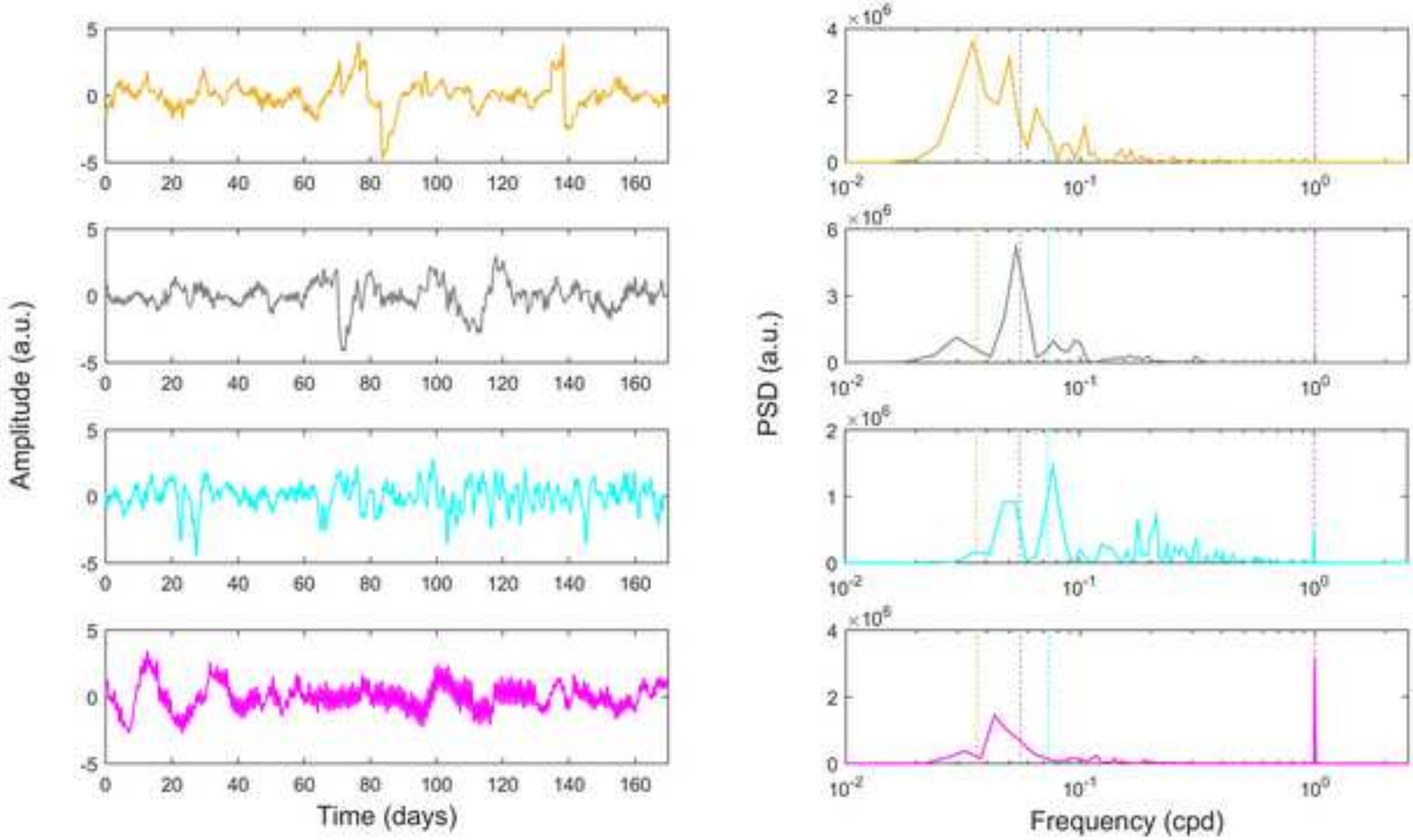

Figure 4

Click here to download high resolution image

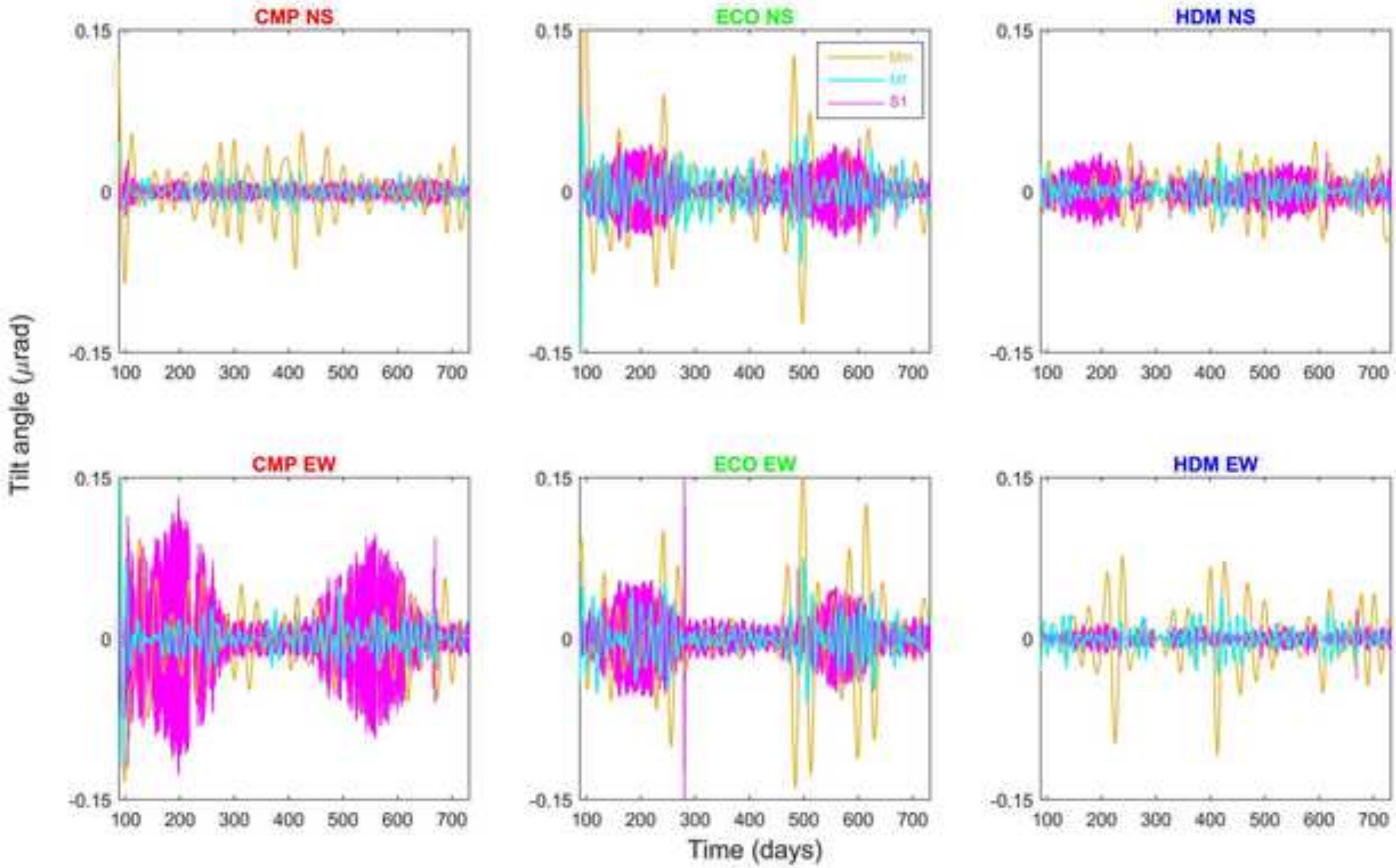

Figure 5
Click here to download high resolution image

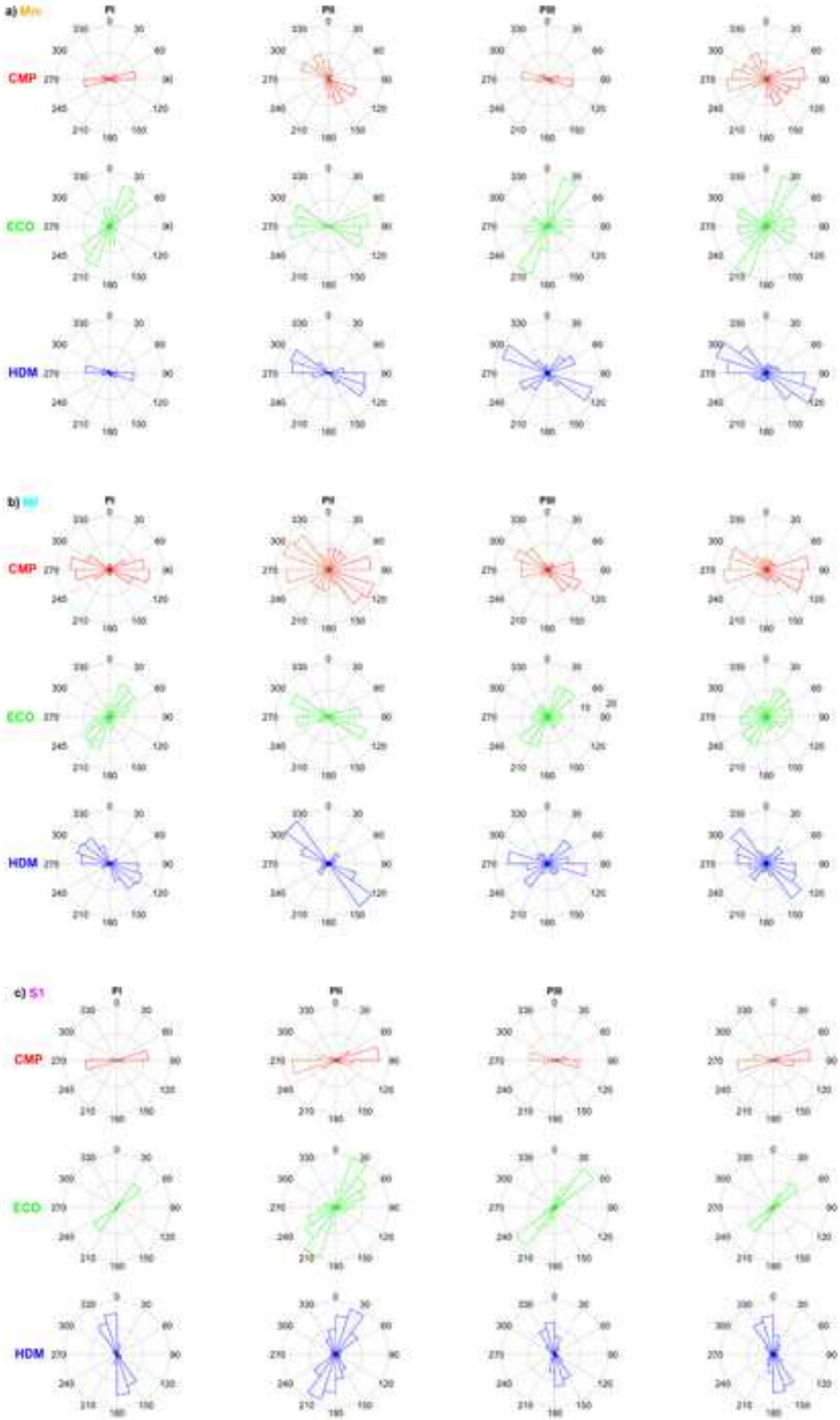

Figure 6
Click here to download high resolution image